CrossMark

electronic reprint

JOURNAL OF
APPLIED
CRYSTALLOGRAPHY

ISSN: 1600-5767
journals.iucr.org/j

A program for refinement of lattice parameters and strain determination using Kossel diffraction patterns

A. Morawiec

J. Appl. Cryst. (2016). **49**, 322–329

IUCr Journals
CRYSTALLOGRAPHY JOURNALS ONLINE

Copyright © International Union of Crystallography

Author(s) of this paper may load this reprint on their own web site or institutional repository provided that this cover page is retained. Republication of this article or its storage in electronic databases other than as specified above is not permitted without prior permission in writing from the IUCr.

For further information see http://journals.iucr.org/services/authorrights.html

JOURNAL OF APPLIED CRYSTALLOGRAPHY

ISSN 1600-5767

A program for refinement of lattice parameters and strain determination using Kossel diffraction patterns

A. Morawiec*

Polish Academy of Sciences, Institute of Metallurgy and Materials Science, Reymonta 25, 30-059 Kraków, Poland. *Correspondence e-mail: nmmorawi@cyf-kr.edu.pl

Received 3 August 2015
Accepted 22 December 2015

Edited by G. Kostorz, ETH Zurich, Switzerland

Keywords: lattice parameters; X-ray diffraction; residual strain; orientation mapping; scanning electron microscopy.

The Kossel diffraction technique is well suited for investigating crystal lattices. Progress in digital recording of images opens the opportunity for simplification and improvement of the examination of Kossel patterns. Such patterns can be processed immediately after recording if appropriate computer programs are available. To provide such a tool, a new Windows-based software for computer-assisted analysis of Kossel patterns has been developed. With its easy-to-operate user interface, the program is intended to facilitate refinement of lattice parameters and determination of elastic strains. The refinement is based on matching experimental and geometrically simulated patterns, whereas the strain is obtained by matching Kossel line profiles in similar experimental patterns. The software is capable of simultaneous handling of multiple patterns.

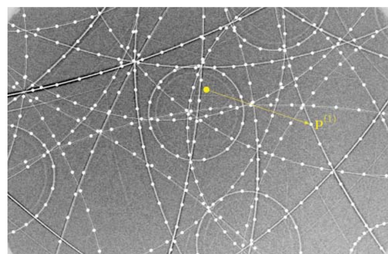

© 2016 International Union of Crystallography

1. Introduction

Kossel diffraction with patterns produced by diverging X-rays is widely known, but this remarkable method of studying crystals is rather rarely used compared to other X-ray techniques. There are a number of different ways of generating Kossel-type patterns, and a variety of experimental setups and pattern acquisition geometries utilizing divergent X-rays. In conventional Kossel diffraction, atoms are excited by a focused electron beam of suitable energy, and the X-ray sources are inside the investigated crystal (Kossel *et al.*, 1935). In the closely related pseudo-Kossel technique, divergent X-rays are generated outside the crystal near its surface in (usually, a surface-deposited layer of) a different material (Lonsdale, 1947). Besides atom excitation by electrons, X-ray Kossel patterns were also obtained using excitation by protons (Geist & Flagmeyer, 1974), synchrotron radiation (Ullrich *et al.*, 1994; Glazer *et al.*, 2004) or lower-energy photons (*e.g.* Despujols & Jordi, 1969; Langer *et al.*, 2005). Other related methods include that of Determann (1937), in which hard X-ray (Kikuchi-like) patterns arise owing to electron-generated *Bremsstrahlung* with a narrow spectrum, or the 'X-ray rotation–tilt' technique (Linnik, 1930; Bauch *et al.*, 2000), in which a rigidly fixed specimen and detector are simultaneously rotated around a sample point with respect to a stationary X-ray source. For reviews of these methods, the interested reader is referred to Langer (2004) and Lider (2011).

Our focus below will be on the conventional Kossel technique. An electron-excited Kossel diffraction pattern is built of a background of *Bremsstrahlung* and lines of characteristic radiation. With a planar detector, the lines have the form of intersecting conic sections. As the locations of the Kossel lines depend on the crystal lattice, the main application of Kossel diffraction is the investigation of lattices. In particular, the

electronic reprint

technique is used for determination of crystal orientations, refinement of lattice parameters and measurement of residual strains.

Early implementations of the Kossel technique suffered from accessibility problems, long exposure times and broad electron probes (resulting in large X-ray sources and low spatial resolution). This has changed with the emergence of electron-probe X-ray microanalysis (EPMA). Applicability of EPMA to Kossel diffraction was demonstrated at the outset by its originator (Castaing, 1951). Related to that development was an upsurge of studies on the Kossel technique and its applications in the 1960s and 1970s [see the accounts of Tixier & Waché (1970) and Yakowitz (1973)]. The contemporary descendant of the Castaing instrument – a scanning electron microscope (SEM) – allows for convenient observations of microstructures, and for easy installation of additional devices (including heating or tensile stages). With a spatial resolution of a few micrometres, Kossel patterns recorded in a SEM can be used for studying individual grains in polycrystalline materials. Besides the Kossel technique, only a few other methods are suitable for local determination of lattice parameters or measurements of third-order (intragranular) residual stresses. Recent decades brought about another development: the digital recording of diffraction patterns. The X-ray films of the past were replaced by phospholuminescent (imaging) plates and by CCD cameras (Ullrich, 1990; Daebritz *et al.*, 1999). This was an important step as digital recording potentially opens the door for automation of pattern analysis. A SEM equipped with a CCD camera is particularly promising in this respect, because it is an easily accessible laboratory-based system, and the images can be processed directly after recording (Langer *et al.*, 2001; Berveiller *et al.*, 2005). The anticipated further progress in digital acquisition and digital image processing is expected to create new opportunities for Kossel microdiffraction. Surprisingly, little has been done to facilitate the analysis of digitally recorded Kossel patterns. The software package that is the subject of this article partly fills this gap.

The package is called *KSLStrain*. Its main functions are the refinement of lattice parameters and the determination of lattice strain from the geometry of Kossel lines. The data needed to perform these computations are the diffraction patterns, the crystal structure with approximate lattice metric, the radiation wavelength and geometric parameters of the experimental setup (approximate location of the pattern center and approximate source-to-detector distance). The algorithms for the refinement are based on a simple geometric description of diffraction: lattice parameters are calculated by matching Kossel lines simulated at Bragg positions to points marking experimental lines. The strain determination procedure also has purely geometric character, but it relies on comparing the geometry of similar experimental patterns, and it is not affected by the complex structure of diffraction lines.

KSLStrain evolved from *TEMStrain*, a program for analysis of the central discs of convergent beam electron diffraction patterns (Morawiec, 2007*b*), and inherits some strengths and deficiencies of the latter. Moreover, indexing subroutines were adapted from a program for indexing of Kikuchi diffraction patterns (Morawiec, 1999). Some features of the package have been presented in conference proceedings (Morawiec *et al.*, 2008; Morawiec, 2014), but these accounts were sketchy. Below, all the main capabilities and limitations of *KSLStrain* are presented. We begin with a description of the geometry of Kossel lines, the indexing procedure and the methods of obtaining lattice parameters; this part explains the essence of the algorithms used in *KSLStrain*. More details of our particular implementation are given in §3.

The physical and experimental aspects of Kossel diffraction are beyond the scope of this article, but for a full picture one needs to recall that not all crystalline structures give conventional Kossel patterns. To allow the observation of Kossel lines, the excitation energy must be sufficiently high so that characteristic X-rays are emitted and, on the other hand, some interplanar spacings must exceed the half-wavelength of the X-rays (see below). By Moseley's law, the excitation energy of $K\alpha$ lines increases with the atomic number Z as $(Z-1)^2 \times 10.2$ eV, and the $K\alpha$ wavelength decreases as $(Z-1)^{-2} \times 121.5$ nm. In practice, the above conditions imply that, to obtain Kossel lines, a crystal must contain (in sufficiently large percent) atoms of an element of the fourth or higher period of the periodic table, and the voltages of 20, 30 and 40 kV correspond to the upper limits of $Z = 45$, 55 and 63, respectively. Thus, the window of applicability of the SEM-based Kossel technique, although not very wide, covers numerous materials of practical importance.

2. Geometry of Kossel lines

Relating a crystal lattice to reflections in a Kossel pattern involves several differently oriented reference frames. The orientations of Cartesian frames, *e.g.* those linked to the specimen, detector and microscope, are described by special orthogonal matrices. More complicated is the essential link between reciprocal lattice vectors representing individual reflections and an external reference frame. Instead of applying one of numerous conventions, *e.g.* the $\mathbf{B}$ matrix of Busing & Levy (1967), we prefer a more general approach: Let (hkl) be the Miller indices of a plane in a direct lattice based on vectors $(\mathbf{a}, \mathbf{b}, \mathbf{c}) = (\mathbf{a}_1, \mathbf{a}_2, \mathbf{a}_3)$. The coordinates of the corresponding reciprocal lattice vector in a Cartesian coordinate system based on vectors $\mathbf{e}_i$ $(i = 1, 2, 3)$ are entries of the one-column matrix

$$\mathbf{h} = A^{-1}\,[h, k, l]^{\mathrm{T}}, \qquad (1)$$

where the matrix A is defined by $A_{ij} = \mathbf{a}_i \cdot \mathbf{e}_j$, *i.e.* A_{ij} is the jth Cartesian component of the ith vector of the lattice basis.

2.1. Plotting a Kossel pattern

There are numerous papers describing algorithms and computer programs for geometric plotting of Kossel lines (*e.g.* Morris, 1968; Bomback & Thomas, 1971; Ullrich *et al.*, 1972; Alex, 1974; Pirouz & Boswarva, 1974; Zhang *et al.*, 1989; Weber, 1997; Langer *et al.*, 1999). Although the algebraic

electronic reprint

characterization of Kossel conics is elementary, it is frequently given using complicated expressions. For this reason and for completeness, we include a simple vectorial description.

The Kossel patterns belong to a larger class that Cowley (1995) named K-line diffraction patterns. The geometry of K-lines follows from the rules of elastic scattering of monochromatic convergent beams. Formally, this geometry is based on the assumption that the wavevectors $\mathbf{k}_0$ of the convergent incident beams have arbitrary directions, but their magnitude is fixed. With individual reflections enumerated by nodes of the crystal reciprocal lattice, the wavevector $\mathbf{k}$ of a reflection corresponding to the node $\mathbf{h}$ is determined by the Laue equation $\mathbf{k} - \mathbf{k}_0 = \mathbf{h}$ and the condition of energy conservation $\mathbf{k}^2 = \mathbf{k}_0^2 = 1/\lambda^2$. These relationships imply the already mentioned basic restriction for crystal diffraction: peaks may arise only for reciprocal lattice vectors satisfying the inequality $|\mathbf{h}| = |\mathbf{k} - \mathbf{k}_0| \leq |\mathbf{k}| + |\mathbf{k}_0| = 2/\lambda$, *i.e.* to observe a reflection, the interplanar spacing $d = 1/|\mathbf{h}|$ must exceed $\lambda/2$. The formula describing K-lines can be easily obtained by noting that $\mathbf{h}$ and $\mathbf{k} + \mathbf{k}_0$ are perpendicular: $\mathbf{h} \cdot (\mathbf{k} + \mathbf{k}_0) = (\mathbf{k} - \mathbf{k}_0) \cdot (\mathbf{k} + \mathbf{k}_0) = \mathbf{k}^2 - \mathbf{k}_0^2 = 0$. Elimination of $\mathbf{k}_0$ from $\mathbf{h} \cdot (\mathbf{k} + \mathbf{k}_0) = 0$ by the Laue equation gives the relationship

$$\mathbf{h} \cdot (\mathbf{k} - \mathbf{h}/2) = 0, \qquad (2)$$

which links the wavevector $\mathbf{k}$ to the reciprocal lattice vector $\mathbf{h}$ without involvement of the arbitrarily directed $\mathbf{k}_0$. Reflections in a K-line diffraction pattern have wavevectors $\mathbf{k}$ satisfying equation (2) and $\mathbf{k}^2 = 1/\lambda^2$. For a given nonzero $\mathbf{h}$, these equations are solved by $\mathbf{k} = \mathbf{h}/2 + \mathbf{l}$, where $\mathbf{l}$ is perpendicular to $\mathbf{h}$ and $\mathbf{l}^2 = 1/\lambda^2 - (\mathbf{h}/2)^2$. Having one vector $\mathbf{l} = \mathbf{l}_0$ of this kind, all wavevectors linked to the reciprocal lattice vector $\mathbf{h}$ are given by the parametric equation

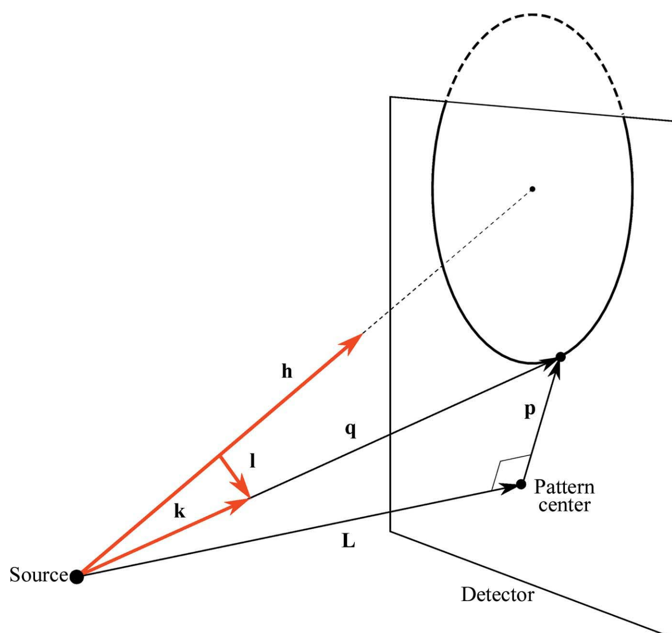

Figure 1
Schematic of vectors involved in the geometric description of a Kossel line. Vectors shown in black (red) are in the direct (reciprocal) space. $\mathbf{L}$ is perpendicular to the detector.

$$\mathbf{k} = \mathbf{h}/2 + \cos(\alpha)\,\mathbf{l}_0 + \sin(\alpha)\,\mathbf{l}_0 \times \mathbf{h}/|\mathbf{h}|, \qquad (3)$$

with α being the parameter. These wavevectors lie on a cone with an axis along $\mathbf{h}$. By equation (2), the cosine of the angle between $\mathbf{k}$ and $\mathbf{h}$ is $(\mathbf{k}/|\mathbf{k}|) \cdot (\mathbf{h}/|\mathbf{h}|) = \lambda/(2d)$, and thus the semi-apex angle of the Kossel cone is complementary to the Bragg angle. An intersection of such cones by a plane (detector) leads to Kossel conics (on a diffraction pattern) (see Fig. 1).

The position of a flat detector is determined by a vector $\mathbf{L}$ perpendicular to its plane and having a magnitude equal to the distance between the X-ray source and the detector. With the initial point of $\mathbf{L}$ at the source, its endpoint on the detector plane is referred to as the pattern center. The observable trace of the reflection linked to the wavevector $\mathbf{k}$ is at

$$\mathbf{q} = \mathbf{L} + \mathbf{L} \times (\mathbf{k} \times \mathbf{L}) \,/\, (\mathbf{k} \cdot \mathbf{L}). \qquad (4)$$

The vector $\mathbf{p} = \mathbf{q} - \mathbf{L}$ with the origin at the pattern center has its endpoint on the Kossel line.

Summarizing, the geometry of the K-lines is determined by $\mathbf{L}$, λ, A and a list of (hkl) planes. A routine for plotting K-line patterns, if written in a high-level programming language, consists of just a few lines expressing equations (1), (3) and (4) plus some code for determining $\mathbf{l}_0$ and inputing data.

2.2. Obtaining lattice data from Kossel lines

Even within the geometric realm, the problems of orientation determination, lattice parameter refinement or strain measurement are much more involved than pattern simulation. Numerous procedures for solving these issues have been devised: from simple charts (*e.g.* Rowlands & Bevis, 1968; Ferran & Wood, 1970) and other geometrical methods (*e.g.* Peters & Oglivie, 1965), to more sophisticated algorithms and computer programs (*e.g.* Heise, 1962; Gielen *et al.*, 1965; Pietrokowsky, 1966; Ryder *et al.*, 1967; Bevis & Swindells, 1967; Morris, 1968; Newman & Shrier, 1970; Fisher & Harris, 1970; Tixier & Waché, 1970; Lutts & Gielen, 1971; Harris & Kirkham, 1971; Harris, 1975; Aristov & Shmytko, 1978). These programs, however, do not take advantage of digital recording of Kossel patterns. Moreover, most of the older approaches are not suitable for analyzing patterns originating from arbitrarily oriented crystallites in polycrystals because they frequently rely on some specific features (*e.g.* points at which more than two Kossel lines intersect each other, points of line tangency or particular 'lenses'), which may be absent or visible only for special crystal orientations.

Analyzing individual grains in polycrystals requires a general approach: the software must allow for arbitrary orientations and make use of various features of diffraction patterns. Ideally, one might consider exploiting complete information *via* 'whole pattern fitting', but using intensities is difficult because line profiles are complicated (Fig. 2). The profiles are influenced by a number of physical factors (electron beam diameter, distribution of electrons in the interaction volume, X-ray absorption, extinction, refraction), the geometry of the experimental setup (position of the crystal with respect to that of the detector and with respect to the

electronic reprint

electron beam) and the digital processing of the pattern (background subtraction method). It is much simpler to rely just on the geometry of Kossel lines.

In the purely geometric approach, it is assumed that the wavelength λ, the approximate direct basis $\mathbf{a}_i$ and the approximate position of the detector $\mathbf{L}$ are known. The analysis of a pattern begins with an assignment of Miller indices to particular Kossel lines. The first step towards indexing is to calculate a single vector $\mathbf{h}$ uniquely characterizing a given Kossel line. This $\mathbf{h}$ can be calculated from, say, N measured $\mathbf{p}^{(i)}$ vectors ($i = 1, \ldots, N$), each of them originating at the pattern center and ending on the line. The following procedure can be used for that purpose: With the direct space vector $\mathbf{x} = \mathbf{h}/|\mathbf{h}|^2$, equation (2) can be written in the form $\mathbf{k} \cdot \mathbf{x} = 1/2$. The vector $\mathbf{k}^{(i)}$ of the wave that arrived at $\mathbf{q}^{(i)} = \mathbf{p}^{(i)} + \mathbf{L}$ is given by $\mathbf{k}^{(i)} = \mathbf{q}^{(i)}/(\lambda|\mathbf{q}^{(i)}|)$. For each of these $\mathbf{k}^{(i)}$ vectors, $\mathbf{x}$ is expected to satisfy

$$\mathbf{k}^{(i)} \cdot \mathbf{x} = 1/2. \tag{5}$$

This is the ith representative of a system of N linear equations with respect to $\mathbf{x}$. The optimal $\mathbf{x}$ is obtained by linear regression: with noncoplanar $\mathbf{k}^{(i)}$, one has $\mathbf{x} = M^{-1}\sum_i \mathbf{k}^{(i)}/2$, where the matrix M is defined by $M = \sum_i \mathbf{k}^{(i)} \otimes \mathbf{k}^{(i)}$ and $\otimes$ denotes the outer product of vectors. Knowing $\mathbf{x}$, one can directly calculate the corresponding $\mathbf{h} = \mathbf{x}/|\mathbf{x}|^2$. Differently than $\mathbf{x}$, which is the least-squares solution of equation (5), the above vector $\mathbf{h}$ has no direct interpretation as 'the best' approximation to the solution of the system $\mathbf{h} \cdot (\mathbf{k}^{(i)} - \mathbf{h}/2) = 0$, but in practice this simple method of obtaining the scattering vector works quite well.

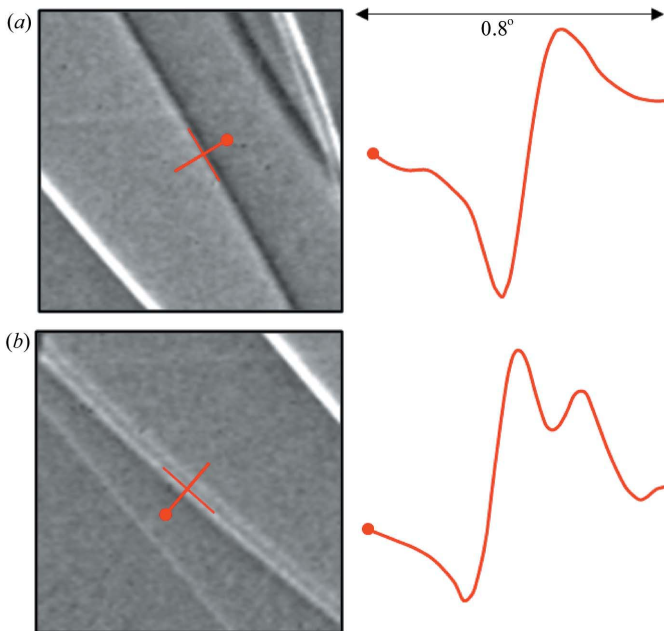

Figure 2
Fragments of Kossel lines of ferrite and their profiles. The reflections are (110) (*a*) and (112) (*b*). The profile in (*a*) demonstrates the bright–dark structure of the line. In (*b*), there are separate peaks of the $K\alpha$ doublet. The profiles were averaged over 0.8° long segments of Kossel lines. The discs are on the convex sides of the lines. The above patterns and those of Figs. 3 and 5 are courtesy of D. Bouscaud (LEM3).

Each conic marked by $\mathbf{p}^{(i)}$ vectors gives a single scattering vector. A set of (at least three) scattering vectors can be used for indexing and to obtain the crystal orientation. This is performed by matching these vectors to low-index vectors of the reciprocal lattice. Formally, the problem can be stated as follows: given two sets, say X and Y, of vectors, determine a rotation carrying X (experimental scattering vectors) to a position approximating a subset of Y (theoretical reciprocal lattice vectors). Solving this problem involves (combinatorial) assignment and (continuous) alignment (see *e.g.* Morawiec, 1999, 2015). The assignment corresponds to indexing of reflections, and the alignment represents fitting of the orientation.

The vectors $\mathbf{k}^{(i)}$ are also used for refining lattice parameters. The definition of these vectors implies that they depend on $\mathbf{L}$, *i.e.* $\mathbf{k}^{(i)} = \mathbf{k}^{(i)}(\mathbf{L})$. Moreover, a small homogeneous deformation F changing a direct space vector $\mathbf{a}$ to $F\mathbf{a}$ causes the inverse change in the reciprocal space, *i.e.* a given reference reciprocal lattice vector $\mathbf{h}$ is transformed to $\mathbf{g} = \mathbf{g}(\mathbf{h}, F) = F^{-1}\mathbf{h}$. The ideal vectors $\mathbf{g}$ and $\mathbf{k}^{(i)}$ are expected to satisfy equation (2), that is $\mathbf{g} \cdot (\mathbf{k}^{(i)} - \mathbf{g}/2) = 0$. Unknown parameters can be determined by minimizing deviations from these equalities. The procedure of obtaining F and $\mathbf{L}$ by minimization of the sum

$$f(F, \mathbf{L}) = \sum\left[\mathbf{g} \cdot (\mathbf{k}^{(i)} - \mathbf{g}/2)\right]^2 \tag{6}$$

is referred to as a 'K-line equation based scheme' or KLEBS (Morawiec, 2007*a*); the summation above is over all marking points of all used conics. The (nine) entries of F determine the (six) strain tensor components and (three) parameters needed for correcting the crystal orientation; the strain tensor is used for calculating the lattice parameters.

3. *KSLStrain*

KSLStrain was created to facilitate the analysis of Kossel diffraction patterns. Operation of the package is controlled *via* a graphical user interface, which simplifies the input and presents results in a convenient form. Besides the simple geometric simulation of Kossel patterns, the program is capable of orientation determination, lattice parameter refinement and strain determination. Neither the refinement nor strain determination requires special crystal orientations. The reliability of the results can be verified by comparing outputs of different strategies available in the package.

As for the limiting factors, the essential computations are based on the geometric theory of diffraction under the assumption of a point-like radiation source, *i.e.* all Kossel cones are assumed to have a common apex. The fine structure of the Kossel lines is used only in profile-based strain determination, when similar patterns are compared. It is also assumed that components of the strain tensor ε and other fitted parameters are small; formally, this is related to application of linear approximations of the type $(I + \varepsilon)^{-1} \simeq (I - \varepsilon)$,

electronic reprint

where I is the identity transformation. Moreover, since line curvatures are used, the program will fail if the lines are nearly straight, *i.e.* when the source-to-detector distance is large compared to the pattern diameter, and in the case of patterns obtained with short wavelengths and having geometry similar to that of Kikuchi patterns.

3.1. Geometric simulation of Kossel patterns

The patterns of Kossel lines are drawn using equations (1), (3) and (4), the user-provided crystal structure and wavelength, and the actual crystal orientation and **L**. The **L** vector is specified in the Cartesian reference frame linked to the detector (with the third axis of the frame perpendicular to the detector plane) by providing the sample-to-detector distance and the coordinates of the pattern center on the detector. The total number of reflections in a geometric simulation of a pattern cannot be larger than 256. Decisions about absences of particular reflections are based on their kinematic intensities and user-provided limits on the largest allowed Miller index and/or the lowest allowed (relative) intensity. The intensities are computed from the X-ray atomic form factors of Waasmaier & Kirfel (1995). For convenience, some parameters of the simulation (orientation parameters, source-to-detector distance) can be modified not only by inputting their values but also by a mouse click. One can also directly display the impact of a given strain tensor component on the geometry of Kossel lines.

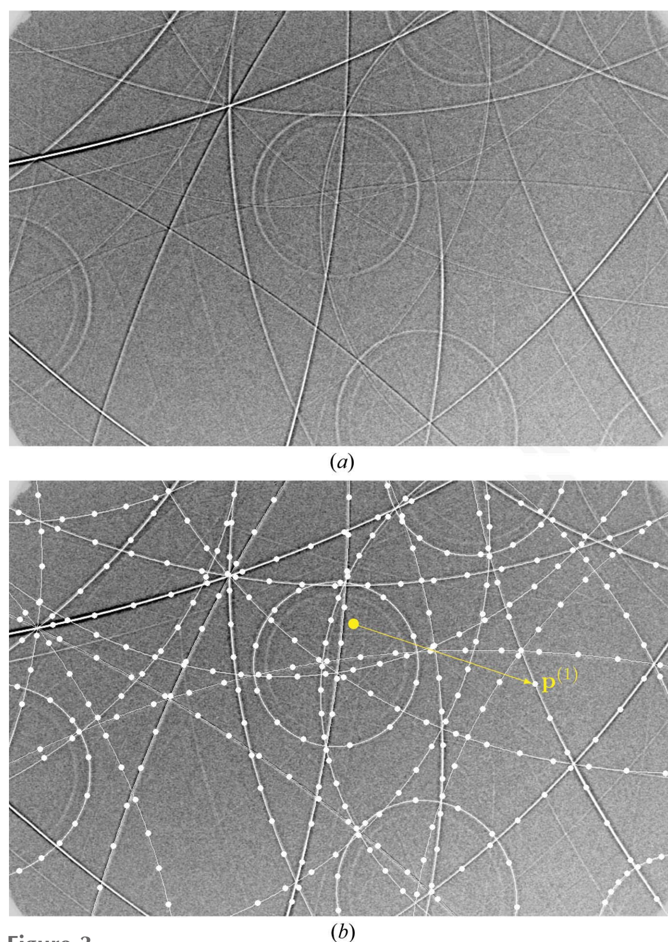

Figure 3
(*a*) Example Kossel diffraction pattern of CuBeAl alloy. (*b*) The same pattern with markers (white discs) of Kossel lines. The approximate location of the pattern center and one of the $\mathbf{p}^{(i)}$ vectors are additionally drawn (in yellow).

3.2. Orientation determination

All steps of pattern interpretation (*i.e.* those beyond the geometric simulation) rely on the locations of markers $\mathbf{p}^{(i)}$ indicating the positions of Kossel lines (see Fig. 3). A marking disc is added by a mouse click. The number of markers per line must be in the range of 3–64; a typical number is about ten. The number of lines marked on a given pattern cannot be larger than 32. The locations of markers can be manually corrected using local profiles of the lines. The profiles are smoothed by averaging over short segments of Kossel lines. With a tool showing a profile, a marker can be moved in steps of 1/10 of a pixel (Fig. 4). The coherency of line marking can be verified by checking the distance of a given marker from a true conic section obtained from all markers of the line (or all other markers of the line).

On the basis of $\mathbf{p}^{(i)}$, λ and **L**, the scattering vectors **h** are obtained using the system of equations (5). The orientation is calculated by matching these vectors to vectors of the reciprocal lattice corresponding to the user-provided crystal structure. The actual indexing is performed by an adapted version of a program designed for obtaining crystal orientations from Kikuchi patterns (Morawiec, 1999). For this reason, the matching procedure involves a redundant step: both the experimental scattering vectors and the reciprocal lattice vectors are normalized to unity. In consequence, the indexing relies on angles between vectors, and vector magnitudes do not play any role. The strategy used for indexing is a form of

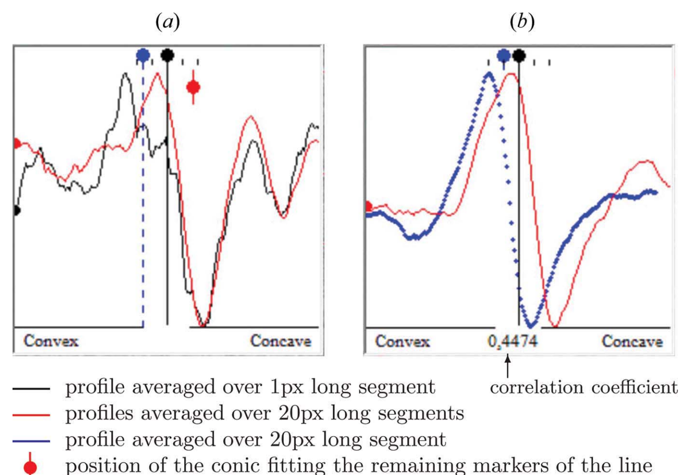

Figure 4
Graphic tools for manual positioning of markers in refinement (*a*) and for matching profiles in strain determination (*b*). The profiles are inverted. The black dashes at the top are separated by one pixel, *i.e.* the complete length of each profile is 20 pixels. The blue elements can be moved to select the point on the Kossel line.

electronic reprint

generalized Hough transform. With small groups of the scattering and reciprocal lattice vectors, the comparison of angles between the vectors indicates candidate orientations. These orientations are accumulated in the space of orientation parameters. The total accumulation near the actual crystal orientation is generally larger than in other parts of the space, and this enables the identification of the crystal orientation and the assignment of Miller indices. The alignment accompanying the indexing involves calculation of the best rotation relating two sets of vectors and the mean orientation (Morawiec, 1998), but this part of the software is separate from the KLEBS-based optimization of orientation parameters in refinement. In practice, as all other parameters are quite accurate, the performance of the indexing routine is determined by the accuracy of the position of the X-ray source with respect to the detector (**L**).

3.3. Refinement of lattice metric

The refinement is based on matching experimental Kossel lines (represented by vectors $\mathbf{p}^{(i)}$) to geometrically simulated conics. Besides the lattice parameters, the parameters of crystal orientation, the sample-to-detector distances and the locations of the pattern centers can also be refined. More precisely, the operator decides about fitting particular components of the tensor ε (= symmetric part of $F - I$), sample-to-detector distances and pattern centers, whereas orientation parameters are always fitted. The program is capable of simultaneous handling of multiple (up to ten) patterns; all these patterns are expected to correspond to the same set of lattice parameters, whereas the orientations and **L** vectors are fitted separately for each pattern. Thus, the number of optimization parameters can reach 66 $[= 6 + 10 \times (3 + 3)]$. In the simplest and usual case, when just one pattern is processed, the number of parameters does not exceed 12.

The current version of the program uses two different optimization procedures: the aforementioned KLEBS and a second, less robust approach, in which distances between intersections of Kossel lines are fitted. The KLEBS method is implemented in two versions: the one described above, *i.e.* the minimization of the function f given by equation (6), and another one minimizing f linearized with respect to small optimization parameters (Morawiec, 2007*a*). In all cases, the search for minima is carried out using the *MINUIT* optimization package (James, 1998).

Crucial for the quality of the refinement is the question of whether the optimization problem is well conditioned, *i.e.* if it has a unique solution, and if the solution is stable with respect to inaccurate (experimental) input data. There are two points of concern. First, the wavelength is correlated to a combination of lattice parameters: the change of λ by the factor ξ to $\xi\lambda$ has the same effect on the geometry of the Kossel lines as the deformation $F = \xi^{-1} I$ applied to the direct lattice in a Cartesian reference frame. Therefore, the wavelength cannot be fitted together with the complete lattice metric. In *KSLStrain*, the user-provided wavelength is assumed to be exact and it is not an optimization parameter; if it needs to be refined, this can be done *via* the equivalence between $\xi\lambda$ and $F = \xi^{-1} I$. Second, as the impact of a small rotation of a crystal about an axis perpendicular to **L** is nearly the same as that of a small shift of the pattern center, there is always a strong correlation between the coordinates of the pattern center and the two parameters of crystal orientation. This is of secondary importance if one looks for lattice parameters or the strain tensor, when the pattern center and orientation parameters are only auxiliary variables. In typical geometry, with the detector diameter comparable to $|\mathbf{L}|$, no other undetectable combinations of the optimization parameters were observed; this was reflected by the absolute values of the correlation coefficients which, in cases other than those considered above, were usually below 0.5, and they rarely exceeded 0.7.

The search for an optimal solution can be complicated by trapping at local minima. For better control of the optimization process, *KSLStrain* allows for display of one-dimensional sections through the objective function. With the patterns considered so far, we have not encountered local minima on these sections, but it must be noted that the KLEBS procedure and single patterns (*i.e.* up to 12 optimization parameters) have mainly been used.

Assuming that the diffraction patterns are free of distortions, the resolution of the refinement of lattice parameters is limited by the widths of the Kossel lines. Some empirical rules for selection of the positions of line markers are given by Bouscaud, Morawiec *et al.* (2014*b*). The actual numbers describing the resolution also depend very much on the material (presence of high-angle reflections) and experimental conditions (**L** and the size of the detector). Results of example resolution tests were given by Bouscaud and co-workers (Berveiller *et al.*, 2014; Bouscaud, Morawiec *et al.*, 2014); *e.g.* for an Ni alloy investigated using the experimental setup described there, the precision of the components of the complete strain tensor was estimated to reach 2×10^{-4} if more than ten Kossel conics per pattern were matched.

3.4. Strain determination

If one has experimental diffraction patterns originating from lattices with similar orientations, the strain can be calculated from the differences between those patterns. The strain determination relies on the lattice parameter refinement, and the resulting strains are relative to the approximately known reference lattice. In other words, in strain determination, lattice parameters obtained from experimental patterns are referred to parameters obtained from other experimental patterns, whereas in mere refinement, absolute lattice parameters are obtained from the strain which needs to be imposed on the user-specified reference lattice, so the simulated line patterns match markers on experimental patterns. Crucial for the accuracy of strain determination is that the locations of the markers of Kossel lines in the investigated pattern are determined precisely using line profiles collected from the reference pattern. (In refinement, to place a marker, an operator must work out which location

electronic reprint

on the profile actually corresponds to the Bragg condition.) The complete procedure for strain determination is as follows:

(1) The reference lattice parameters are refined using the experimental reference patterns.

(2) The reference lattice parameters and (reference) profiles corresponding to these parameters are saved.

(3) The saved reference profiles are used to put markers of lines in the investigated patterns.

(4) These new positions are then used to refine lattice parameters corresponding to the investigated patterns and to obtain the lattice strain with respect to the reference lattice parameters. See Fig. 5.

KSLStrain facilitates fitting intensity profiles along directions perpendicular to Kossel lines. In the second step of the above procedure, the marking points can be selected automatically. With this approach, some of these points may turn out to be unsuitable (*e.g.* markers at low-angle intersections of Kossel lines) and they must be manually removed. The third step can also be done semi-automatically: the software puts the markers at locations giving the largest correlation coefficient between the reference profiles and the profiles in the investigated pattern, but the results of this procedure must be checked by the operator and, if needed, individual profiles can be matched manually.

Tests on simulated patterns indicate that the resolution of the profile-based approach is considerably better than that of the geometry-based refinement (Morawiec, 2014). As in the case of the refinement, it depends on the material and experimental conditions.

Note that the above profile-based approach is similar to strain determination by digital image correlation. The difference is that no direct correlation of Kossel patterns is possible as a lattice strain moves particular points of Kossel lines in a complicated manner. One could envisage determination of strain by using conventional image correlation applied to the Hough transforms of Kossel patterns, but at present this seems to be computationally too costly.

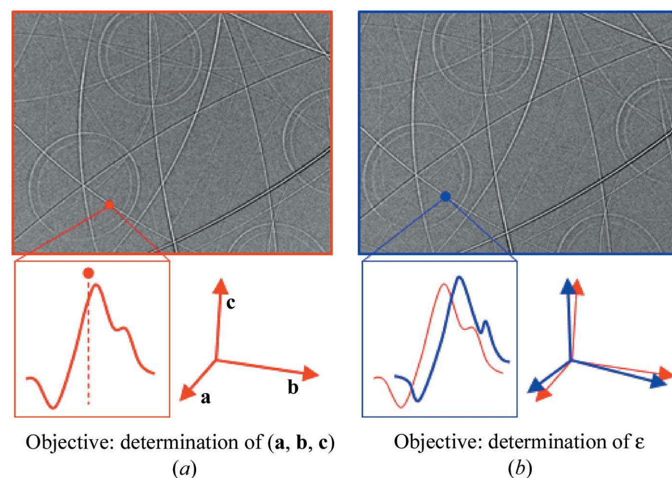

Figure 5
Schematic of the strain determination procedure. The lattice parameter refinement is limited by the accuracy of positioning the line markers as in (*a*). The reference (red) objects in (*b*) originate from (*a*). In strain determination, the markers in the investigated pattern (*b*) are positioned using the profiles collected from the reference pattern (*a*).

3.5. Language, platform, availability and documentation

The *KSLStrain* program was written in Fortran90 (essential computations) and VB6 (user interface). It runs on 32 bit personal computers under Microsoft Windows (XP or later) operating systems, with the Windows display-scale variable set to default 96 d.p.i. ('Small icons' setting). The input diffraction patterns must be in the form of 8 or 24 bit grayscale bitmap files of dimensions not smaller than 512 × 512 pixels and of a width (in pixels) divisible by 4. A 4.6 MB self-extracting executable file can be downloaded from http://imim.pl/personal/adam.morawiec/A_Morawiec_Web_Page/downloads.html. The documentation is limited to HTML-formatted help files.

4. Concluding remarks

In response to progress in digital recording of Kossel diffraction images a new software package for analysis of such patterns has been developed. Its main applications are the refinement of lattice parameters and determination of lattice strains. The refinement is based purely on the geometry of Kossel lines, and comparison of line profiles is used to calculate strain.

Prospects for advancement of the SEM-based Kossel technique depend on the automation of pattern acquisition and on further automation of pattern analysis. The latter step requires a self-explanatory and easy-to-manipulate user interface minimizing the input an operator needs to provide, and *KSLStrain* partly resolves the issue. For true automation, however, additional software for effective and accurate detection of the conics would be needed, and progress in this matter has been slow.[1] As of today, we believe that to create a program accurately detecting most of the conics, one will have to include information about the relationships between particular scattering vectors. This means in practice that conic detection will be inherently combined with orientation determination. A more complete program might also be capable of simulating profiles of Kossel lines on the basis of physically justified arguments. Such simulation would expand the list of input parameters, but assuming it provides profiles similar to those observed experimentally, this addition may considerably improve the accuracy of lattice parameter refinement.

A relatively small fraction of published software is directly used or adapted, as other researchers look for different

[1] Early in the development of *KSLStrain*, an attempt was made to add automatic positioning of marking points (using a generalized Hough transform under the assumption that approximate **L** and magnitudes |**h**| are known). That software turned out to be slow and, more importantly, the detection was inaccurate so manual verification and correction of markers was necessary. Similar speed and accuracy were reached in a recent attempt made independently by Kudłacz (2014). In the meantime, accounts with opposite, rather optimistic, conclusions have been published by Maurice & Fortunier (2008) and Bauch *et al.* (2011), but we are not aware of any applications of these programs.

electronic reprint

functionalities or prefer to rely on their own creations. However, newer programs do not only duplicate some features of their predecessors. Usually, they use improved algorithms, they have more capabilities and, ultimately, they become parts of full-scale, well maintained, user-friendly systems. *KSLStrain* – although complete in its form – should be seen as a step toward more sophisticated and more automatic analysis of Kossel diffraction patterns.

Acknowledgements

The author is grateful to D. Bouscaud of LEM3, Metz, and K. Kudłacz of IMMS for their comments and contributions, and also to E. Bouzy as the paper was written during a stay at LEM3 on his invitation. The work was supported in part by the National Science Center based on decision No. DEC-2012/06/M/ST8/00449.

References

Alex, V. (1974). *Krist. Tech.* **9**, 169–174.
Aristov, V. V. & Shmytko, I. M. (1978). *J. Appl. Cryst.* **11**, 662–668.
Bauch, J., Henschel, F. & Schulze, M. (2011). *Cryst. Res. Technol.* **46**, 450–454.
Bauch, J., Ullrich, H. J. & Reiche, D. (2000). *Cryst. Res. Technol.* **35**, 473–478.
Berveiller, S., Dubos, P., Inal, K., Eberhardt, A. & Patoor, E. (2005). *Mater. Sci. Forum*, **490–491**, 159–165.
Bevis, M. & Swindells, N. (1967). *Phys. Status Solidi*, **20**, 197–212.
Bomback, J. L. & Thomas, L. E. (1971). *J. Appl. Cryst.* **4**, 356–370.
Bouscaud, D., Berveiller, S., Pesci, R., Patoor, E. & Morawiec, A. (2014). *Adv. Mater. Res.* **996**, 45–51.
Bouscaud, D., Morawiec, A., Pesci, R., Berveiller, S. & Patoor, E. (2014). *J. Appl. Cryst.* **47**, 1699–1707.
Busing, W. R. & Levy, H. A. (1967). *Acta Cryst.* **22**, 457–464.
Castaing, R. (1951). PhD thesis, University of Paris, France, ONERA No. 55.
Cowley, J. M. (1995). *Diffraction Physics*. Amsterdam: Elsevier.
Daebritz, S., Langer, E. & Hauffe, W. (1999). *J. Anal. At. Spectrom.* **14**, 409–412.
Despujols, J. & Jordi, F. (1969). *Vth International Congress on X-ray Optics and Microanalysis*, edited by G. Moellenstedt & K. H. Gaukler, pp. 412–414. Berlin: Springer.
Determann, H. (1937). *Schr. Naturforsch. Ges. Danzig Neue Folge*, **20**, 5–7.
Ferran, G. & Wood, R. A. (1970). *J. Appl. Cryst.* **3**, 419–421.
Fisher, D. G. & Harris, N. (1970). *J. Appl. Cryst.* **3**, 305–313.
Geist, V. & Flagmeyer, R. (1974). *Phys. Status Solidi A*, **26**, K1–K3.
Gielen, P., Yakowitz, H., Ganow, D. & Ogilvie, R. E. (1965). *J. Appl. Phys.* **36**, 773–782.
Glazer, A. M., Collins, S. P., Zekria, D., Liu, J. & Golshan, M. (2004). *J. Synchrotron Rad.* **11**, 187–189.
Harris, N. (1975). *J. Mater. Sci.* **10**, 279–289.
Harris, N. & Kirkham, A. J. (1971). *J. Appl. Cryst.* **4**, 232–240.
Heise, B. H. (1962). *J. Appl. Phys.* **33**, 938–941.
James, F. (1998). *MINUIT. Function Minimization and Error Analysis.* CERN, Geneva, Switzerland.
Kossel, W., Loeck, V. & Voges, H. (1935). *Z. Phys.* **94**, 139–144.
Kudłacz, K. (2014). Unpublished work.
Langer, E. (2004). PhD thesis, TU Dresden, Germany.
Langer, E., Daebritz, S., Hauffe, W. & Haschke, M. (2005). *Appl. Surf. Sci.* **252**, 240–244.
Langer, E., Daebritz, S., Schurig, C. & Hauffe, W. (2001). *Appl. Surf. Sci.* **179**, 45–48.
Langer, E., Kurt, R. & Daebritz, S. (1999). *Cryst. Res. Technol.* **34**, 801–816.
Lider, V. V. (2011). *Crystallogr. Rep.* **56**, 169–189.
Linnik, W. (1930). *Z. Phys.* **61**, 220–226.
Lonsdale, K. (1947). *Philos. Trans. R. Soc. London Ser. A*, **240**, 219–250.
Lutts, A. & Gielen, P. (1971). *J. Appl. Cryst.* **4**, 242–250.
Maurice, C. & Fortunier, R. (2008). *J. Microsc.* **230**, 520–529.
Morawiec, A. (1998). *J. Appl. Cryst.* **31**, 818–819.
Morawiec, A. (1999). *J. Appl. Cryst.* **32**, 788–798.
Morawiec, A. (2007*a*). *Ultramicroscopy*, **107**, 390–395.
Morawiec, A. (2007*b*). *J. Appl. Cryst.* **40**, 618–622.
Morawiec, A. (2014). *Adv. Mater. Res.* **996**, 52–57.
Morawiec, A. (2015). *IOP Conf. Ser. Mater. Sci. Eng.* **82**, 012008.
Morawiec, A., Pesci, R. & Lecomte, J. S. (2008). *Ceram. Trans.* **201**, 163–170.
Morris, W. G. (1968). *J. Appl. Phys.* **39**, 1813–1823.
Newman, B. A. & Shrier, A. (1970). *J. Appl. Cryst.* **3**, 280–281.
Peters, E. T. & Oglivie, R. E. (1965). *Trans. Met. Soc. AIME*, **233**, 89–95.
Pietrokowsky, P. (1966). *J. Appl. Phys.* **37**, 4560–4571.
Pirouz, P. & Boswarva, I. M. (1974). *Phys. Status Solidi A*, **26**, 407–415.
Rowlands, P. C. & Bevis, M. F. (1968). *Phys. Status Solidi*, **26**, K25–K28.
Ryder, P. L., Haelbig, H. & Pitsch, W. (1967). *Microchim. Acta*, **Suppl. II**, 123–132.
Tixier, R. & Waché, C. (1970). *J. Appl. Cryst.* **3**, 466–485.
Ullrich, H. J. (1990). *Mikrochim. Acta*, **101**, 19–24.
Ullrich, H. J., Schlaubitz, M., Friedel, F., Spann, T., Bauch, J., Wroblewski, T., Garbe, S., Gaul, G., Knoechel, A., Lechtenberg, F., Rossmanith, E., Kumpat, G. & Ulrich, G. (1994). *Nucl. Instrum. Methods Phys. Res. Sect. A*, **349**, 269–273.
Ullrich, H. J., Thiele, K., Daebritz, S., Schreiber, H., Goetze, K. & Feldhofer, F. (1972). *Krist. Tech.* **7**, 1153–1168.
Waasmaier, D. & Kirfel, A. (1995). *Acta Cryst.* A**51**, 416–431.
Weber, S. (1997). *J. Appl. Cryst.* **30**, 85.
Yakowitz, H. (1973). *The Divergent Beam (Kossel) X-ray Method and Its Uses in Measuring Strain Contours in an Individual Grain of Fe-3 Weight Percent Si Transformer Sheet*. Washington, DC: National Bureau of Standards.
Zhang, J. Z., Fan, D. P., Ren, H. & Zhou, B. (1989). *Chinese Sci. Bull.* **34**, 549–552.

electronic reprint